Towards hot electron mediated charge exchange in hyperthermal energy ion–surface interactions

2010 J. Phys.: Condens. Matter 22 084010

(http://iopscience.iop.org/0953-8984/22/8/084010)

J. Phys.: Condens. Matter **22** (2010) 084010 (5pp) doi:10.1088/0953-8984/22/8/084010

Towards hot electron mediated charge exchange in hyperthermal energy ion–surface interactions

M P Ray[1], R E Lake[1], L B Thomsen[2], G Nielson[2], O Hansen[2,3], I Chorkendorff[2] and C E Sosolik[1]

[1] Department of Physics and Astronomy, Clemson University, Clemson, SC 29634, USA
[2] CINF Center for Individual Nanoparticle Functionality, Department of Physics, Nano DTU, Technical University of Denmark, DK-2800 Kongens Lyngby, Denmark
[3] Department of Micro- and Nanotechnology, Technical University of Denmark, DTU, Nanotech Building 345 East, DK-2800 Kongens Lyngby, Denmark

E-mail: sosolik@clemson.edu

Received 1 July 2009, in final form 8 September 2009
Published 4 February 2010
Online at stacks.iop.org/JPhysCM/22/084010

Abstract
We have made Na^+ and He^+ ions incident on the surface of solid state tunnel junctions and measured the energy loss due to atomic displacement and electronic excitations. Each tunnel junction consists of an ultrathin film metal–oxide–semiconductor device which can be biased to create a band of hot electrons useful for driving chemical reactions at surfaces. Using the binary collision approximation and a nonadiabatic model that takes into account the time-varying nature of the ion–surface interaction, the energy loss of the ions is reproduced. The energy loss for Na^+ ions incident on the devices shows that the primary energy loss mechanism is the atomic displacement of Au atoms in the thin film of the metal–oxide–semiconductor device. We propose that neutral particle detection of the scattered flux from a biased device could be a route to hot electron mediated charge exchange.

(Some figures in this article are in colour only in the electronic version)

1. Introduction

Desorption induced by electronic transitions (DIET) is a subject of fundamental [1–4] and practical [5] importance in the field of surface science. The general framework for DIET processes was outlined in 1964 by Menzel, Gomer, and Redhead [6, 7]. One route to initiating DIET is by the use of femtosecond lasers, which have been shown to induce desorption in a large class of adsorbate systems and promote chemical reactions which cannot proceed by thermal heating [8].

In laser-induced DIET processes, substrate excitation is manifested as an internal flux of excited electrons toward the surface. Inelastic scattering of these excited electrons with an adsorbate redistributes the energy into various degrees of freedom, and if enough energy is transferred into the center-of-mass translational motion of the adsorbate, desorption may occur. The high density of excited electrons created by femtosecond lasers can result in desorption induced by multiple electronic transitions (DIMET) [9] or could be used to mediate hot electron femtochemistry at surfaces (HEFatS) [10].

An alternative method proposed for HEFatS involves the use of a metal–insulator–metal (MIM) or metal–oxide–semiconductor (MOS) device [10, 11]. With an ideal MOS device, it may be possible to tune hot electrons to a desired resonance of an adsorbate system by tuning the bias voltage across the device. Such devices have been constructed and characterized and are candidates for future HEFatS experiments [11]. We present measurements of internal hot electron yields in MOS devices induced by hyperthermal energy ions as well as an analysis of the ion–surface scattering dynamics.

2. Experimental techniques

The MOS devices utilized in the measurements reported here were mounted in a unique ultrahigh vacuum (UHV) ion

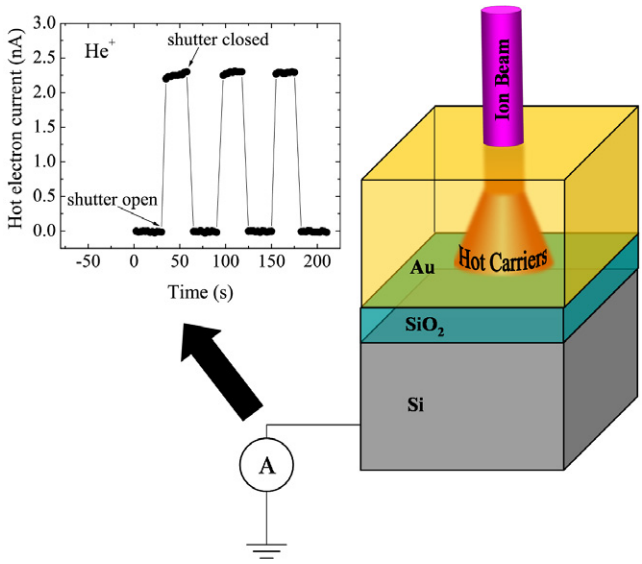

Figure 1. Cross section of the MOS device under ion bombardment. The plot shows the hot electron current measured through the MOS device in response to three periods of bombardment by 600 eV He^+.

scattering system [12]. The ion source consists primarily of a Colutron G-2 ion gun[4] with a gas source for He^+ production and a home-built source [13] that incorporates a commercially available alkali-doped aluminosilicate ion emitter[5] for Na^+ production. The ions are scattered from the target in a two-tier UHV chamber that houses various surface analysis tools, two scattered particle detectors, and a six-axis manipulator stage. The ion detector is located in the lower tier of the scattering chamber and lies in the plane with the incident ion beam. The ion detector uses a 180° electrostatic analyzer (ESA) and channel electron multiplier to detect ions with an energy resolution of 1%.

The beam exposure targets are large area ultrathin film MOS devices [11] shown schematically in figure 1. The exposed surface of these devices consists of a 10 nm Au layer on top of a 1 nm Ti wetting layer. The metal layers are separated from an n-doped Si(100) substrate by 5 nm of thermally grown silicon dioxide.

The room temperature devices were exposed to a beam of Na^+ ions which were scattered from the surface and detected using the ESA. A typical spectrum is shown in figure 3, where the scattered intensity is plotted versus the scattered ion energy. For all spectra, intensity is determined by summing the counts during a 5 s dwell time at a given pass energy E and normalizing by a factor of $1/E$ to account for the transmission function of the ESA.

In addition to ion detection, a neutral particle detector (NPD) can be used to detect neutral atoms. The NPD is used to obtain velocity-resolved neutralization probabilities for studying charge transfer in the Na^+–MOS system. Using this detector and a combination of beam pulsing and standard time-of-flight techniques, the total scattered flux (ions and neutrals) and the neutrals-only scattered flux can be measured [14]. The ratio of the integrated neutrals-only intensity to the integrated total intensity is taken as a measure of the neutralization probability (P_0). This system has been successfully used previously with single-crystal metal targets [15, 16].

In addition to scattering measurements, electron–hole pair excitations caused by the ion impacts can also be probed using MOS devices. Charge excitations induced by the incident ion beam were measured at both the front metal and back Ohmic contacts of each exposed device. Each device was electrically connected to the sample stage and shielded to limit the beam exposure to a small portion (8.0 mm^2) of the 1 cm^2 Au top layer. A typical current response under a He^+ beam exposure is shown in the inset of figure 1. He^+ was chosen for these measurements because it has relatively high velocity at low energy and thus creates a highly nonadiabatic ion–solid interaction that results in excited electrons. All hot electron measurements were made with the ion beam focused at normal incidence to the device surface, and it was verified that photons emanating from the ion source created no measurable signal. Multiple, identically prepared devices were exposed to beams of He^+ and the observed current response was consistent between the devices used. The I–V characteristics of each device were measured both pre- and post-exposure and compared to known results [11] to verify that the device had not been altered due to beam effects.

The internal hot carrier current was measured through the back contact for each species as a function of the incident beam energy. The internal excitation yield, Γ_{ie}, was used to quantify the kinetic energy or velocity-dependent effects for each device, where Γ_{ie} is defined as the ratio of the magnitude of the back-face current to the difference in the front and back current responses. Defining the yield in this way accounts for possible contributions from secondary or exoelectrons, although such effects were found to be minimal. Results for Γ_{ie} are shown in figure 2 for He^+ as a function of the incident beam energy.

3. Results and discussion

3.1. Surface assisted electron excitations

Emission of electrons in this energy regime has historically been treated within the context of simple models that account for kinetic electron excitations (KEE) by treating the target, in this case our top metal layer, as an idealized Fermi gas. Within such a model, a velocity threshold for kinetic electron emission, dependent only on the Fermi energy and the surface work function, can be found [17, 18]. For our work, we substitute the internal barrier height of the MOS device for the surface work function and obtain the following threshold velocity expression:

$$v_{th} = \frac{1}{2} v_f \left[\left(1 + \frac{\phi_b}{E_f} \right)^{1/2} - 1 \right], \qquad (1)$$

where ϕ_b is the barrier height and v_f and E_f are the Fermi velocity and Fermi energy for Au, respectively. The values for ϕ_b and E_f were chosen to be 4.2 and 5.5 eV. The vertical

[4] Colutron Research Corporation, Boulder, CO.
[5] HeatWave Labs, Inc., Watsonville, CA.

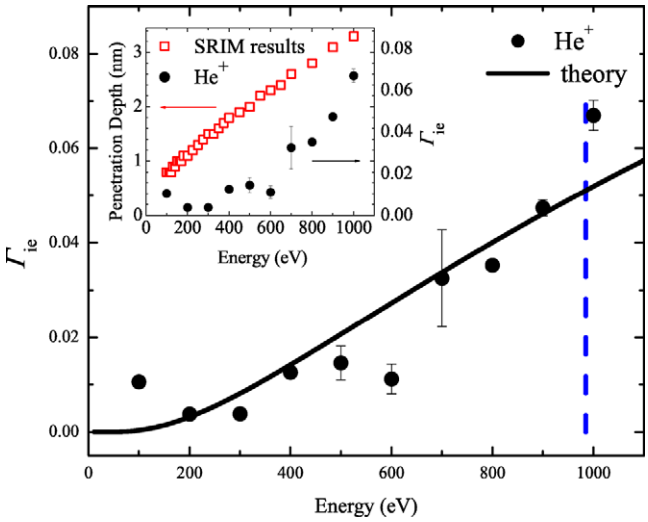

Figure 2. Current yield as a function of incident ion energy for He^+. The solid line is the theoretical result from a model that describes charge carrier excitations caused by ion–surface interactions. The vertical dashed line represents the threshold for charge carrier excitations using a free electron model of a metal below which there should be no excitations. The inset shows penetration depth as a function of the incident He^+ energy.

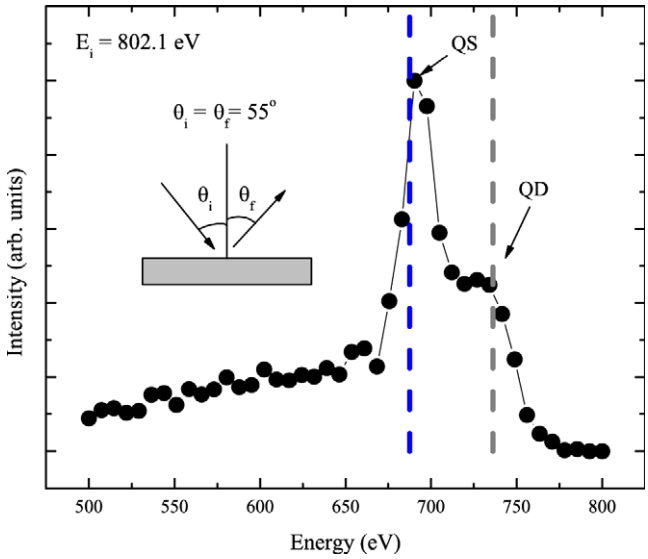

Figure 3. A representative spectrum for 802.1 eV Na^+ scattering from a MOS ($Au/SiO_2/n$-Si) device. The inset depicts the scattering geometry used in the experiment. The dashed vertical lines represent the energy loss due to quasi-single (QS) and quasi-double (QD) collisions as predicted within the binary collision model. A line is drawn between successive data points to guide the eye.

dashed line shown in figure 2 represents the threshold energy value obtained for He^+, and it is clear that our experimentally observed excitations occur below this threshold.

Previous studies on subthreshold behavior in ion–solid interactions have attributed measured responses to four distinct mechanisms: electron promotion, multi-electron processes, Auger excitations, and nonadiabatic interactions between the ion and the surface [19–24]. For our measurements we can rule out the first two mechanisms as the incident energies employed are too low for close-collision-induced promotion and He^+ is too simple (low Z) for multi-electron effects to arise. Additionally, no Auger transitions analogous to those seen in previous systems exist for our projectile–target combinations. Therefore, we are left to consider the role that nonadiabatic interactions play in creating our subthreshold signal responses. However, given the penetrating nature of the ions used here, it is also reasonable to suspect that depth-dependent effects could be present, especially for our thin Au films. To address this issue and determine the range of the ion species into the metal layer, we have used the simulations TRIM and SRIM [25]. The ranges obtained for He^+ indicate that the mean depth obtained is less than 5.0 nm or half the thickness of the Au thin film. To determine whether there is a correlation between penetration depth and the current yield, SRIM results are compared to the measured yield results. From this comparison it is clear that both increase as a function of the beam energy as shown in figure 2. This is a correlation in energy-dependent behavior, and hence this does not indicate a causal relationship between the penetration depth and the measured yield. Preliminary measurements using incident species other than He^+ agree with the theoretical model outlined in the manuscript and further suggest that the hot electrons are generated at the surface of the device as we have proposed [26].

Prior measurements of subthreshold electron emission external to a solid target have utilized the Falcone–Sroubek theory which is an extension of the concept of linear stopping power that is based on nonadiabatic interactions between the projectile ion and the metal atoms [19, 20, 27, 28]. Nonadiabaticity in this model is included via a time-varying ion–surface interaction that is characterized by the projectile velocity v, the potential V, and a distance-dependent parameter γ that accounts for the presence of the surface [28]. Applying this model to our system, we can obtain a probability of kinetic electron excitation P_{KEE} above the MOS barrier as

$$P_{\mathrm{KEE}} = A\rho^2 V^2 \ln\left(\exp\left(-\frac{\pi\phi_{\mathrm{b}}}{2\gamma v}\right)+1\right). \qquad (2)$$

The parameters A and ρ correspond to the collection efficiency of the MOS device and the target density of states, respectively. If we interpret our measurements of Γ_{ie} as a direct measurement of this probability, we obtain the line shown in figure 2. Here we have constrained γ to be ~1.0 au, which is its expected value within this model. In order to obtain good agreement with the data, the value of the prefactor $A\rho^2V^2$ is set as 0.539 ± 0.049 and measurements are currently under way to compare this prefactor across different incident species [26].

3.2. Hyperthermal energy ion scattering spectroscopy

Spectra were obtained for Na^+ ions scattered from the surface of MOS devices at an incident energy of 802.1 eV. The Na^+ ions were scattered specularly from the MOS target at an incident angle of $\theta_{\mathrm{i}} = 55°$ with respect to the surface normal. In the representative data taken at $\theta_{\mathrm{f}} = 55°$ in figure 3, two well-defined peaks that correspond to significant energy losses are clearly resolved.

In order to determine the energy loss peaks seen in figure 3, we employ the binary collision approximation (BCA) which assumes that energy and momentum are conserved in the scattering events. Given the small de Broglie wavelength of the incident ionic projectiles ($\lesssim$0.02 Å) used here, it is reasonable to assume that a scattering trajectory can be broken down into one or more single collisions between the incident ion and individual atoms at the surface. Using these assumptions the final scattered energies can be predicted. Previous measurements for alkali ion–surface scattering from single-crystal surfaces in this incident energy range have revealed similar features indicative of single and successive ion–atom collisions [29, 30]. Our approach relies on the kinematic factor, $k_{\pm}$, which gives the ratio of the final and incident energies of the projectile ion, E_f and E_i, following a single collision with a target surface atom:

$$k_{\pm}(\mu, \theta_{TSA}) = \frac{E_f}{E_i} = \frac{\mu^2}{(1+\mu)^2} \times \left[\cos\,\theta_{TSA} \pm \left(\frac{1}{\mu^2} - \sin^2\theta_{TSA}\right)^{1/2}\right]^2. \quad (3)$$

This factor is a function of the projectile-to-target mass ratio $\mu = m_{proj}/m_{target}$ and the total scattering angle, $\theta_{TSA} = 180° - \theta_i - \theta_f$. Two possible solutions for this factor, differing in sign, are indicated. However, for light ($\mu < 1$) atom–surface scattering systems such as Na–Au(MOS), we need only consider the k_+ solution.

Figure 3 shows the kinematic factor (vertical dashed line) for a single collision between a Na atom and a Au atom. Also shown is the factor for a double collision (vertical dashed line), which we define to be forward scattering of the Na from one Au into an angle of 90° followed by a second forward scattering collision from $\theta_i = 90°$ into the final angle of the detector. We observe excellent agreement between the single-scattering kinematic factor and one of the most intense peaks present in the data. Similar agreement is also seen for the double-collision expression. Therefore we conclude that the primary trajectories which arise in the scattering of Na^+ from a MOS device are the quasi-single (QS) and quasi-double (QD) trajectories.

3.3. Hot electron mediated charge exchange

Applying a bias across an MOS device creates a flux of electrons that is driven from the Si substrate toward the surface of the ultrathin Au film. This flux of electrons could be used to drive chemical reactions at surfaces [10, 11]. We suggest that hyperthermal energy ion scattering measurements can be used to probe the alteration in the electronic structure at the surface of the MOS device. The agreement between the BCA and the scattering data implies that the energy of the incident ion is initially dissipated into the displacement of Au atoms and shows no evidence for hot electron excitation. Therefore we propose that alterations in the charge transfer could be measured for specific trajectories such as the QS and QD in hyperthermal energy alkali scattering from a biased MOS device.

Na^+ was scattered from biased (+5 V) and unbiased devices with the specular scattering angle $\theta_i = \theta_f = 55°$. Due to the significant 0.17 eV difference in energy between the bare ionization potential of a Na ion and the Au surface work function [31], it is expected that ions scattered from the unbiased device will not be resonantly neutralized. As the Na^+–Au image interaction will further shift the Na 3s ionization level upon the ion's approach to the surface, it could be possible to detect an enhanced neutral fraction that is correlated with the applied bias voltage on a device. To date, we observe no such change in the neutral fraction when a +5 V bias is applied, and additional measurements will be performed as a function of bias voltage and incident ion species and energy to further explore this proposed concept.

4. Conclusions

In conclusion we present experimental data for internal hot electron yield in MOS devices induced by hyperthermal energy He^+ bombardment. Measured yields were well described by nonadiabatic kinetic electron emission theory. An analysis of the energy loss of Na ions scattered from the devices was also presented and fitted with the BCA. Excellent agreement with the BCA indicates that ion kinetic energy is primarily deposited into the lattice rather than the electronic system of the Au film, and we propose that neutralization measurements for scattering from a biased device could provide a path toward hot electron mediated charge exchange.

References

[1] Ho W 1988 *Comments Condens. Matter Phys.* **13** 293
[2] Avouris P and Walkup R E 1989 *Annu. Rev. Phys. Chem.* **40** 173
[3] Zhou X L, Zhu X Y and White J M 1991 *Surf. Sci. Rep.* **13** 73
[4] Ramsier R D and Yates J T Jr 1991 *Surf. Sci. Rep.* **12** 243
[5] Madey T E, Czyzewski J J and Yates J T Jr 1975 *Surf. Sci.* **49** 465
[6] Menzel D and Gomer R 1964 *J. Chem. Phys.* **41** 3311
[7] Redhead P A 1964 *Can. J. Phys.* **42** 886
[8] Brandbyge M, Hedegard P, Heinz T F, Misewich J A and Newns D M 1995 *Phys. Rev.* B **52** 6042
[9] Misewich J A, Heinz T F and Newns D M 1992 *Phys. Rev. Lett.* **68** 3737
[10] Gadzuk J W 1996 *Phys. Rev. Lett.* **76** 4234
[11] Thomsen L B, Nielsen G, Vendelbo S B, Johansson M, Hansen O and Chorkendorff I 2007 *Phys. Rev.* B **76** 155315
[12] Ray M P, Lake R E, Moody S A, Magadala V and Sosolik C E 2008 *Rev. Sci. Instrum.* **79** 076106
[13] Peale D R, Adler D L, Litt B R and Cooper B H 1989 *Rev. Sci. Instrum.* **60** 730
[14] Kimmel G A and Cooper B H 1993 *Rev. Sci. Instrum.* **64** 672
[15] Kimmel G A and Cooper B H 1993 *Phys. Rev.* B **48** 12164
[16] Sosolik C E, Hampton J R, Lavery A C, Cooper B H and Marston J B 2003 *Phys. Rev. Lett.* **90** 013201
[17] Baragiola R 1993 *Nucl. Instrum. Methods Phys. Res.* B **78** 223
[18] Baragiola R A, Alonso E V, Ferron J and Oliva-Florio A 1979 *Surf. Sci.* **90** 240
[19] Lakits G, Aumayr F, Heim M and Winter H 1990 *Phys. Rev.* A **42** 5780

[20] Lorincik J and Sroubek Z 2000 *Phys. Rev.* B **62** 16116
[21] Baragiola R A, Alonso E V and Florio A O 1979 *Phys. Rev.* B **19** 121
[22] Yarmoff J A, Liu T D, Qiu S R and Sroubek Z 1998 *Phys. Rev. Lett.* **80** 2469
[23] Sroubek Z, Chen X and Yarmoff J A 2006 *Phys. Rev.* B **73** 045427
[24] Yarmoff J A, Than H T and Sroubek Z 2002 *Phys. Rev.* B **65** 205412
[25] Biersack J and Haggmark L 1980 *Nucl. Instrum. Methods* **174** 257
[26] Ray M P, Lake R E, Thomsen L B, Nielsen G, Hansen O, Chorkendorff I and Sosolik C E 2009 *Phys. Rev.* B submitted
[27] Falcone G and Sroubek Z 1989 *Phys. Rev.* B **39** 1999
[28] Lorincik J and Sroubek Z 2000 *Nucl. Instrum. Methods* B **164/165** 633
[29] DiRubio C A, McEachern R L, McLean J G and Cooper B H 1996 *Phys. Rev.* B **54** 8862
[30] Ray M P, Lake R E and Sosolik C E 2009 *Phys. Rev.* B **79** 155446
[31] Kawano H 2008 *Prog. Surf. Sci.* **83** 1